

# Rapid simulated hydrologic response within the variably saturated near surface

Brian A. Ebel\* and  
Keith Loague

Department of Geological and  
Environmental Sciences, Stanford  
University, Stanford, CA 94305-2115,  
USA

\*Correspondence to:

Brian A. Ebel, Department of  
Geological and Environmental  
Sciences, Stanford University,  
Stanford, CA 94305-2115, USA.  
E-mail: bebel32@stanford.edu

## Abstract

Column and field experiments have shown that the hydrologic response to increases in rainfall rates can be more rapid than expected from simple estimates. Physics-based hydrologic response simulation, with the Integrated Hydrology Model (InHM), is used here to investigate rapid hydrologic response, within the variably saturated near surface, to temporal variations in applied flux at the surface boundary. The factors controlling the speed of wetting front propagation are discussed within the Darcy–Buckingham conceptual framework, including kinematic wave approximations. The Coos Bay boundary-value problem is employed to examine simulated discharge, pressure head, and saturation responses to a large increase in applied surface flux. The results presented here suggest that physics-based simulations are capable of representing rapid hydrologic response within the variably saturated near surface. The new InHM simulations indicate that the temporal discretization and measurement precision needed to capture the rapid subsurface response to a spike increase in surface flux, necessary for both data-based analyses and evaluation of physics-based models, are smaller than the capabilities of the instrumentation deployed at the Coos Bay experimental catchment. Copyright © 2007 John Wiley & Sons, Ltd.

**Key Words** rapid hydrologic response; Coos Bay; integrated hydrology model; InHM

## Introduction

The general objective in preparing this short communication was to further discuss and demonstrate the utility of hydrologic-response simulation for effectively examining field observations and, in certain situations, for making queries beyond the measured data (also see Loague and VanderKwaak, 2004; Ebel and Loague, 2006; Loague *et al.*, 2006). The specific objective of this effort was to further assess the type of hydrologic-response data needed to rigorously test or evaluate both physics-based models and the theories upon which these models are based. This paper is focused on understanding rapid simulated hydrologic response within the variably saturated near surface. Many studies have demonstrated that preferential flow, via high permeability pathways, can be an important source of rapid hydrologic response (e.g. Beven and Germann, 1982; Clothier, 2002; Nimmo, 2007). The simulations in this study consider only matrix-flow-dominated rapid hydrologic response, of the type observed within the unsaturated near surface during the field and laboratory experiments conducted by Torres *et al.* (1998); Rasmussen *et al.* (2000); Renshaw *et al.* (2003), and Meyles *et al.* (2006).

The effort reported here is grounded in Horton's *measure and model* approach (see Beven, 2004). The data is from an experimental catchment in coastal Oregon near Coos Bay (Montgomery *et al.*, 1997); the model is the comprehensive physics-based *Integrated Hydrology Model* (InHM) developed by VanderKwaak (1999). The comprehensive, physics-based classification denotes a model that is based on solution (often numerical) to the fully coupled, complete set of partial differential equations that describe hydrologic response across the spatially variable surface and within the variably saturated subsurface (see Loague and VanderKwaak, 2004). A *comprehensive* model should represent all significant physical processes.

Received 30 March 2007  
Accepted 2 October 2007

A *physics-based* model should employ parameters that have a physical interpretation or significance (i.e. can be measured) and processes that are developed and tested within a scientific framework (after Beven, 1989a). It is important to establish that the effort reported herein was not designed to (i) promote one hydrologic-response model over another, (ii) denigrate any underlying modeling technique, or (iii) endorse or refute any rapid response theories (e.g. pressure waves (Torres *et al.*, 1998)).

## Rapid Hydrologic Response

### Controlling factors

An explanation of the factors controlling the rate of hydrologic response benefits from an examination of the governing flow equations (i.e. assuming Darcy's law and continuum mechanics are valid). The 3D saturated homogeneous isotropic flow equation is:

$$K \frac{\partial^2 h}{\partial x^2} + K \frac{\partial^2 h}{\partial y^2} + K \frac{\partial^2 h}{\partial z^2} = S_s \frac{\partial h}{\partial t} \quad (1)$$

where  $x$ ,  $y$  and  $z$  denote Cartesian coordinates,  $K$  is the saturated hydraulic conductivity [ $L T^{-1}$ ],  $h$  is the hydraulic head [ $L$ ],  $S_s$  is the specific storage [ $L^{-1}$ ], and  $t$  is time [ $T$ ]. The specific storage is defined as:

$$S_s = \rho g(\alpha + n\beta) \quad (2)$$

where  $\rho$  is the density of water [ $M L^{-3}$ ],  $g$  is gravitational acceleration [ $L T^{-2}$ ],  $\alpha$  is the porous media compressibility [ $M L^{-1} T^{-2}$ ],  $n$  is the porosity [ $L^3 L^{-3}$ ], and  $\beta$  is the fluid compressibility [ $M L^{-1} T^{-2}$ ]. The 3D unsaturated homogeneous isotropic (nonlinear) flow equation is:

$$\frac{\partial}{\partial x} \left( K(\psi) \frac{\partial \psi}{\partial x} \right) + \frac{\partial}{\partial y} \left( K(\psi) \frac{\partial \psi}{\partial y} \right) + \frac{\partial}{\partial z} \left( K(\psi) \frac{\partial \psi}{\partial z} + 1 \right) = C(\psi) \frac{\partial \psi}{\partial t} \quad (3)$$

where  $K(\psi)$  is the characteristic function for hydraulic conductivity [ $L T^{-1}$ ],  $\psi$  is the pressure head [ $L$ ], and  $C(\psi)$  is the specific moisture capacity [ $L^{-1}$ ]. The specific moisture capacity is defined as:

$$C(\psi) = \frac{d\theta}{d\psi} \quad (4)$$

where  $\theta$  is soil water content [ $L^3 L^{-3}$ ]. Perusal of Equations (1) and (3) shows that the three factors controlling the rate of hydrologic response (i.e. the  $\frac{\partial h}{\partial t}$  and  $\frac{\partial \psi}{\partial t}$  terms in Equations (1) and (3), respectively) are: (i) the hydraulic conductivity,  $K$  or  $K(\psi)$  (directly proportional); (ii) the hydraulic gradient,  $\frac{\partial h}{\partial x}$  or  $\frac{\partial \psi}{\partial z} + 1$  (directly proportional); and (iii) the storage,  $S_s$  or  $C(\psi)$  (inversely proportional). In general, increases in the hydraulic conductivity and/or the gradient or decreases in the storage result in a more rapid hydrologic response.

The work reported here is focused on the physics of the unsaturated zone as represented by Equation (3). The

three main factors controlling the rates of hydrologic response (i.e. (i)–(iii) above) are present in many simplifications of the flow equations (see Colbeck, 1972; Beven, 1981, 1982; Smith, 1983; Charbeneau, 1984). For example, both Smith (1983) and Charbeneau (1984) approximate the wetting front velocity as:

$$v = \frac{[K(\theta_1) - K(\theta_2)]}{(\theta_1 - \theta_2)} \quad (5)$$

where  $v$  is the velocity [ $L T^{-1}$ ],  $\theta_1$  is the soil water content behind the wetting front [ $L^3 L^{-3}$ ],  $\theta_2$  is the soil water content ahead of the wetting front [ $L^3 L^{-3}$ ],  $K(\theta_1)$  is the hydraulic conductivity at  $\theta_1$  [ $L T^{-1}$ ], and  $K(\theta_2)$  is the hydraulic conductivity at  $\theta_2$  [ $L T^{-1}$ ]. On the basis of the assumption that the initial hydraulic conductivity or flux ahead of the wetting front is zero, Warrick *et al.* (1971) and Beven (1982, 1989b) estimate the wetting front velocity as:

$$v = \frac{K(\theta_s)}{(\theta_s - \theta_2)} \quad (6)$$

where  $\theta_s$  is the soil water content at the surface [ $m^3 m^{-3}$ ] and  $K(\theta_s)$  is the hydraulic conductivity [ $L T^{-1}$ ] at  $\theta_s$ . The numerator in both Equations (5) and (6) is hydraulic conductivity, which can be replaced with the surface flux (e.g. rainfall); the denominator in both Equations (5) and (6) represents storage. Assuming a steady infiltration capacity at the surface,  $K(\theta_s)$  is equal to the applied flux. The hydraulic gradient in both Equations (5) and (6) is assumed to be unity (i.e. matric potential gradients are zero, gravity dominates) and therefore does not change.

Smith (1983), when comparing transient estimates of wetting front position, found good agreement between the kinematic wave-based Equation (5) and numerical solution to the more rigorous Equation (3). Renshaw *et al.* (2003) successfully matched estimates of wetting front velocities from the kinematic wave-based Equation (6) with observed values. As noted by Smith (1983) and Beven (1989b), consistent with Equations (5) and (6), rainfall rates near the saturated conductivity of soils with wet initial conditions (i.e. very little storage) result in large wetting front velocities. Torres *et al.* (1998); Williams *et al.* (2002), Renshaw *et al.* (2003), and Meyles *et al.* (2006) each cite high rainfall rates on soils with wet initial conditions and steep hydraulic conductivity functions as the conditions necessary conditions for rapid observed hydrologic responses, which they term *pressure waves*. For a steep characteristic curve the value of pressure head is very sensitive to changes in soil water content or hydraulic conductivity. The distinction between Equations (5) and (6) is that with Equation (5) the hydraulic conductivity function (with respect to soil water content) must increase steeply for the wetting front to advance rapidly. On the basis of comparisons with numerical simulations from Equation (3), Smith (1983) and Smith *et al.* (2002) determined that Equation (5) is more robust than Equation (6) for estimating the wetting front arrival time.

## Coos Bay Experimental Catchment

Three intensely monitored sprinkling experiments were conducted at the 860 m<sup>2</sup> Coos Bay experimental catchment (CB1) between 1990 and 1992 (see Anderson *et al.*, 1997a,b, 2002; Montgomery *et al.*, 1997; Torres *et al.*, 1998; Ebel *et al.*, 2007b). The CB1 experiments facilitate observation and simulation-based characterization of the integrated and distributed surface and near-surface hydrologic response. Analyses of the CB1 data has included descriptions of the spatial and temporal dynamics within the variably saturated subsurface (see Montgomery *et al.*, 1997, 2002; Torres *et al.*, 1998), runoff generation (see Anderson *et al.*, 1997b; Montgomery *et al.*, 1997; Montgomery and Dietrich, 2002), and solute transport/weathering (see Anderson *et al.*, 1997a,b, 2002; Anderson and Dietrich, 2001). Major themes that emerge from the aforementioned CB1 data studies are that the unsaturated zone and the fractured bedrock both play important roles in the overall hydrologic response of the catchment.

An important observation from the CB1 measurements is that the near-surface hydrologic response was rapid for both the sprinkling experiments and for natural rainfall events. Torres *et al.* (1998) and Montgomery *et al.* (2002) both attribute the rapid pressure head response CB1 to the advance of a *pressure wave* within the near surface. Torres *et al.* (1998) compared the observed (gleaned from tensiometers nested with depth) and estimated (with the approach from Warrick *et al.* (1971)) wetting front velocities, finding the former 15 times faster. Torres *et al.* (1998) also found that the observed (from tensiometers) time to quasi-steady state was 2–4 times faster than estimated with an empirical approach given by Horton (1940). Montgomery *et al.* (2002) found that the observed piezometric response was 100 times faster than estimated from a simple wetting front approximation (i.e. sprinkling rate divided by the soil porosity). In contrast to the rapid (relative to simple approximations) observed pressure responses reported by Torres *et al.* (1998) and Montgomery *et al.* (2002), the analyses by Anderson *et al.* (1997a) found that deuterium spiked water detected in subsurface lysimeters moved approximately at the spatially variable sprinkling rates divided by the soil water content behind the wetting front, which is in agreement with the Warrick *et al.* (1971) approximation for solute transport.

## Physics-Based Hydrologic Response Simulation, Cb1 Experiment 2

Considering the success of kinematic wave approximations at representing hydrologic response, one could question the need for comprehensive physics-based simulation: especially since the uncertainty associated with the typical application of a deterministic-conceptual model is well known (see Beven, 2006). At CB1, the complicating factors that prevent models which are based on simplifying assumptions from effectively representing distributed hydrologic response (see Ebel and Loague, 2006) include:

(i) hysteretic soil water retention curves, (ii) spatially and temporally variable sprinkling rates, (iii) complex subsurface soil and geology, and (iv) nonuniform initial conditions. The extensive site characterization (Anderson *et al.*, 1997a,b; Montgomery *et al.*, 1997, 2002; Torres *et al.*, 1998; Montgomery and Dietrich, 2002; Ebel *et al.*, 2007b), combined with recent physics-based simulation efforts (see Ebel and Loague, 2006; Ebel *et al.*, 2007a,c), provide a foundation for investigating rapid hydrologic response at CB1. The new InHM simulations reported herein for the second CB1 sprinkling experiment are heuristic in nature in that no soil water content data exists and that no pressure head measurements were made during a natural storm that augmented the sprinkling (5/27/1990 2:00 A.M. to 7:00 A.M.). InHM is described by VanderKwaak (1999) and VanderKwaak and Loague (2001); past applications of InHM include VanderKwaak and Loague (2001); Loague *et al.* (2005); Heppner *et al.* (2006, 2007); Jones *et al.* (2006); Mirus *et al.* (2007); Ebel *et al.* (2007c); Ran *et al.* (2007), and Smerdon *et al.* (2007).

For the simulation-based effort reported here, discharge (at the upper weir), pressure head, and saturation estimates (at selected points) are used to examine the hydrologic response at CB1 for sprinkling experiment number 2. The locations of the upper weir and the monitoring points used in this study are shown in Figure 1. The boundary value problem used for the new CB1 simulations is the same as reported by Ebel *et al.* (2007c), with one exception. During the period when the natural storm augments sprinkling, a spatially uniform sprinkling and rainfall flux (10 min temporal resolution) replaces the kriged sprinkling rate snapshots (9–15 h temporal resolution) employed by Ebel *et al.* (2007c) as the surface boundary condition. The 10 min discretization sprinkling and rainfall rates are the mean of the rates measured in three automated rain gages (see Ebel *et al.*, 2007b). During the high-intensity spike, the three automated rain

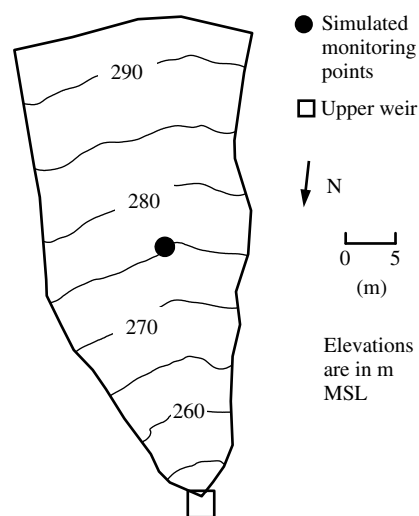


Figure 1. Location of the upper weir and simulated monitoring points within the CB1 catchment. The simulated monitoring points consist of a vertical series, collocated in  $x$  and  $y$ , of points from the soil surface to the soil–saprolite geologic interface

gages recorded rates of 18.3, 16.8, and 15.2 mm h<sup>-1</sup>, giving an average of 16.8 mm h<sup>-1</sup>. The range in recorded rainfall rates, even at the small CB1 site, illustrates the considerable uncertainty in estimating rainfall (see Sieck *et al.*, 2007). The finer temporal discretization in the flux used for the surface boundary condition used in this study facilitates examining the effect that the short duration rainfall spike had on the near-surface hydrologic response.

### Integrated response

The integrated hydrologic response (i.e. discharge) represents the combination of many hydrologic processes and flowpaths that interact to produce the observed runoff. The integrated response of the CB1 catchment to sprinkling and natural rainfall during the second sprinkling experiment is shown in Figure 2(a) and (b). Figure 2(a) illustrates a cause and effect relationship between the observed sprinkling and rainfall hyetograph and the observed upper weir discharge hydrograph for experiment 2. Also shown in Figure 2(a) is the InHM-simulated discharge hydrograph for sprinkling experiment 2, facilitating an observed *versus* simulated comparison of the integrated hydrologic response. As shown in Figure 2(a), the simulated hydrograph is, in general, a good representation of the observed response; the peak is slightly overestimated and the rising and recession limbs are both somewhat lagged. Figure 2(b) is an enlargement of a small section of the record shown in Figure 2(a), illustrating the rapid simulated response in discharge related to the rainfall spike. As shown in Figure 2(b), the local peak in the simulated discharge response, driven by the rainfall spike, is 11 min after the initiation of the spike and is largely dissipated within another 10 min. The magnitude of the perturbation in discharge to the rainfall spike is on the order of 0.01–0.02 l s<sup>-1</sup>, which is below the detection limit of the stage-monitoring equipment that was installed at the CB1 upper weir. The 10-min resolution of the observed discharge record did not detect the response to the rainfall spike. It is worth noting that the most of the rapid (but small magnitude) discharge response shown in Figure 2(b) results from sprinkling and rainfall that falls on a limited saturated area just upslope of the CB1 upper weir (see Montgomery *et al.*, 1997; Ebel *et al.*, 2007b). The small magnitude discharge response shown in Figure 2(b) is, of course, not the only upper weir discharge response to the rainfall spike. The rainfall spike contributes to the simulated (and observed) upper weir discharge for hours afterwards as the rainfall spike infiltrates, moves vertically through the unsaturated soil column, and then advances downslope through the fractured weathered bedrock (see Montgomery and Dietrich, 2002). Clearly all the runoff generation could not occur for the entire CB1 catchment (either simulated or observed) over a period of 20 min in response to the rainfall spike. It is our opinion that the ambiguity in employing discharge alone to determine catchment response time

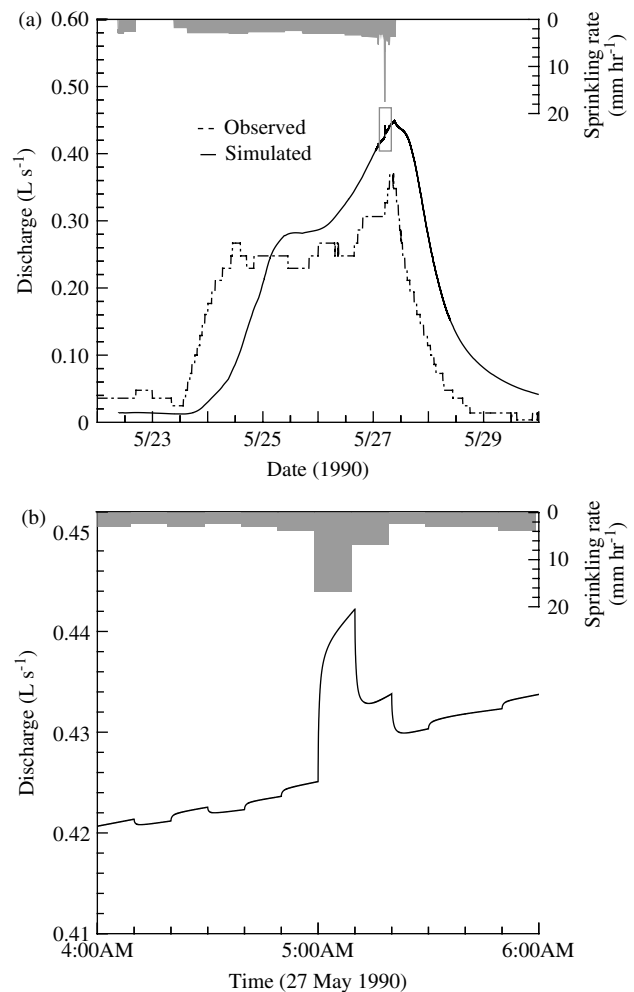


Figure 2. (a) Observed *versus* InHM-simulated discharges for the entire second CB1 sprinkling experiment. The hyetograph of sprinkling and rainfall is shown on the vertical axis. (b) Subset of the InHM-simulated discharge during the second sprinkling experiment; note that the gray box in (a) shows the subset time range for the simulated discharge in (b). The rapid simulated discharge response to the natural rainfall rate increase is evident

is a limitation of the integrated response (i.e. discharge) in data-based or simulation-based hydrologic investigations.

### Distributed response

In contrast to the integrated response, the distributed response consists of point measurements (e.g. pressure head, saturation) that reflect the localized hydrologic processes. Figure 3(a) shows temporal snapshots of simulated pressure head at the simulated monitoring points. The five profiles are for (i) the initial condition at the start of sprinkling experiment 2, (ii) exactly at the initiation of the rainfall spike, (iii) 10 min after the initiation of the rainfall spike (i.e. when the spike ends), (iv) 30 min after the initiation of the rainfall spike, and (v) 2 h after the initiation of the rainfall spike (i.e. at 7:00 A.M. when the tensiometer measurements were taken). The initial condition profile shows the wetting front from a natural storm preceding sprinkling experiment 2. Figure 3(b) is an enlargement of a section of the profile shown in Figure 3(a), which facilitates distinguishing between the

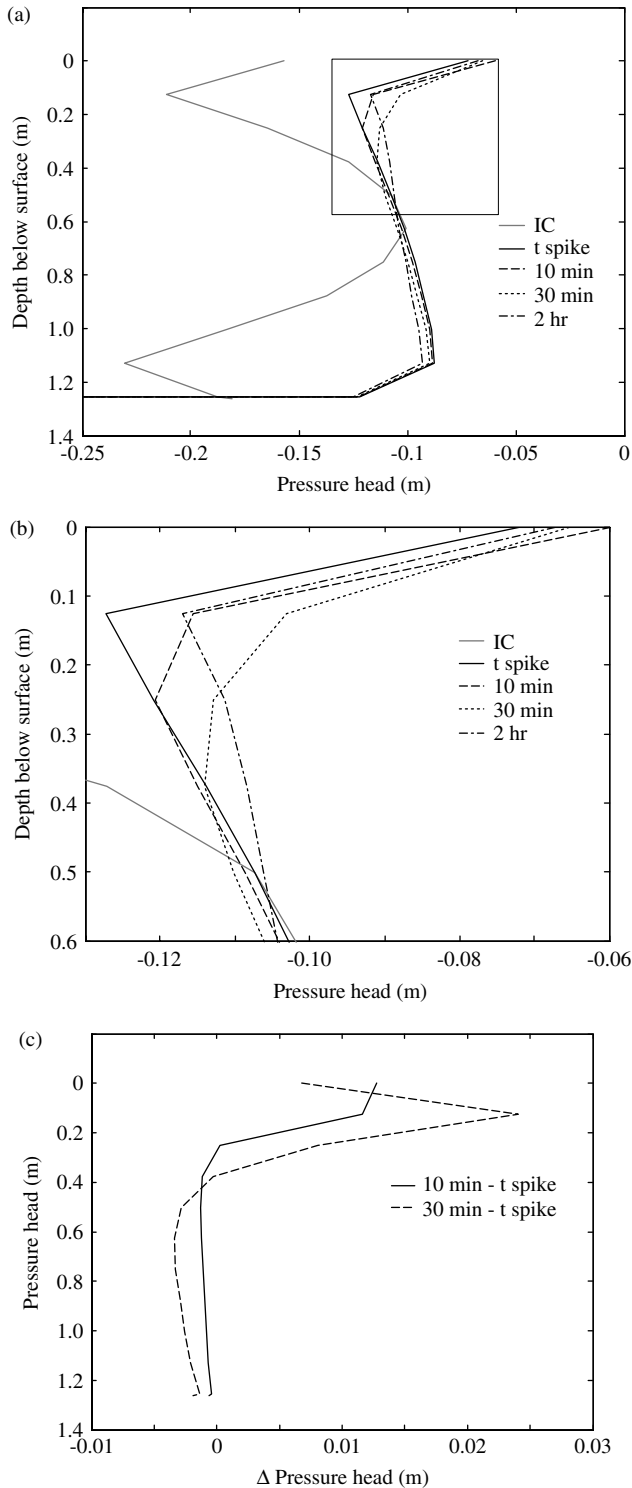


Figure 3. (a) Time snapshots of simulated pressure head profiles with depth for the simulated monitoring points for the second CB1 sprinkling experiment initial conditions (IC), at the initiation of the natural rainfall rate spike, 10 min after the rainfall spike initiated (also the cessation of the rainfall spike), 30 min after the rainfall spike initiated, and 2 h after the rainfall spike initiated. (b) Subset of the profiles shown in (a); note that the box in (a) shows the depth range of the subset. (c) Depth profiles of the differences between the pressure heads at the simulated monitoring points at the rainfall spike initiation and the time snapshots from 10 and 30 min after the rainfall spike

five profiles. The small and rapid magnitudes of the simulated pressure head response are a result of the extremely

steep wetting soil water retention curves (Torres *et al.*, 1998; Ebel *et al.*, 2007c). Because the flux rate at the surface during the brief rainfall spike is only  $17 \text{ mm h}^{-1}$ , compared to the estimated saturated hydraulic conductivity of the soil of  $1200 \text{ mm h}^{-1}$ , the additional rainfall flux from the spike is easily accommodated with only a couple of centimeters of increase in pressure head. Figure 3(c) shows the changes in the simulated pressure head throughout the profile at 10 and 30 min after the initiation of the rainfall spike. The largest change in pressure head throughout the profile is 0.024 m at 0.125 m below the surface at approximately 30 min after the initiation of the rainfall spike. The 30 min surface pressure head declines very rapidly because of the hysteretic behavior of the soil water retention curve (i.e. transitioning to a drying curve on a scanning curve that is less steep than the wetting curve).

Figure 4(a) shows temporal snapshots of simulated saturation at the simulated monitoring points. The profiles in Figure 4(a) are for the same times as in Figure 3(a). Figure 4(b) is an enlargement of a section of the profile shown in Figure 4(a), which facilitates distinguishing between the five profiles. Given the magnitude of the rainfall spike, the changes in saturation needed to accommodate the increased flux at the surface are small owing to the steep hydraulic conductivity function and the large saturated hydraulic conductivity of the soil. The simulated saturations in Figure 4(a) and (b) remain far from full saturation. Owing to the high (i.e.  $0.5 \text{ m}^3 \text{ m}^{-3}$ ) porosity of the soil at the site (Montgomery *et al.*, 1997; Ebel *et al.*, 2007c), much of the increased flux from the rainfall spike goes to storage. The maximum difference in the simulated saturation for a given depth within the profile is  $0.042 \text{ m}^3 \text{ m}^{-3}$  at the surface (resulting from the boundary condition) 10 min after the initiation of the rainfall spike. Simulated saturations at depth are less than at the surface because water moves into storage as it infiltrates. Figure 4(c) shows the changes in simulated saturation throughout the profile at 10 and 30 min after the initiation of the rainfall spike.

Two hours after the initiation of the rainfall spike (7:00 A.M., 27 May 1990), corresponding to the first tensiometer measurements made after the spike (Torres *et al.*, 1998), the maximum simulated pressure head and saturation differences are, respectively, 0.010 m and  $0.0137 \text{ m}^3 \text{ m}^{-3}$ . Torres *et al.* (1998) noted that the 7:00 A.M. measurements showed no response (beyond instrument noise) to the rainfall spike. Given the rapid and small nature of the pressure head and saturation disturbances, it is not surprising that detection of the rainfall spike was not possible with the observations from the instrumentation and temporal discretization used (nearly 20 years ago) to capture the hydrologic response at CB1 during experiment 2.

## Discussion

The results from the new set of InHM simulations for CB1 reported here support the conclusions of previous

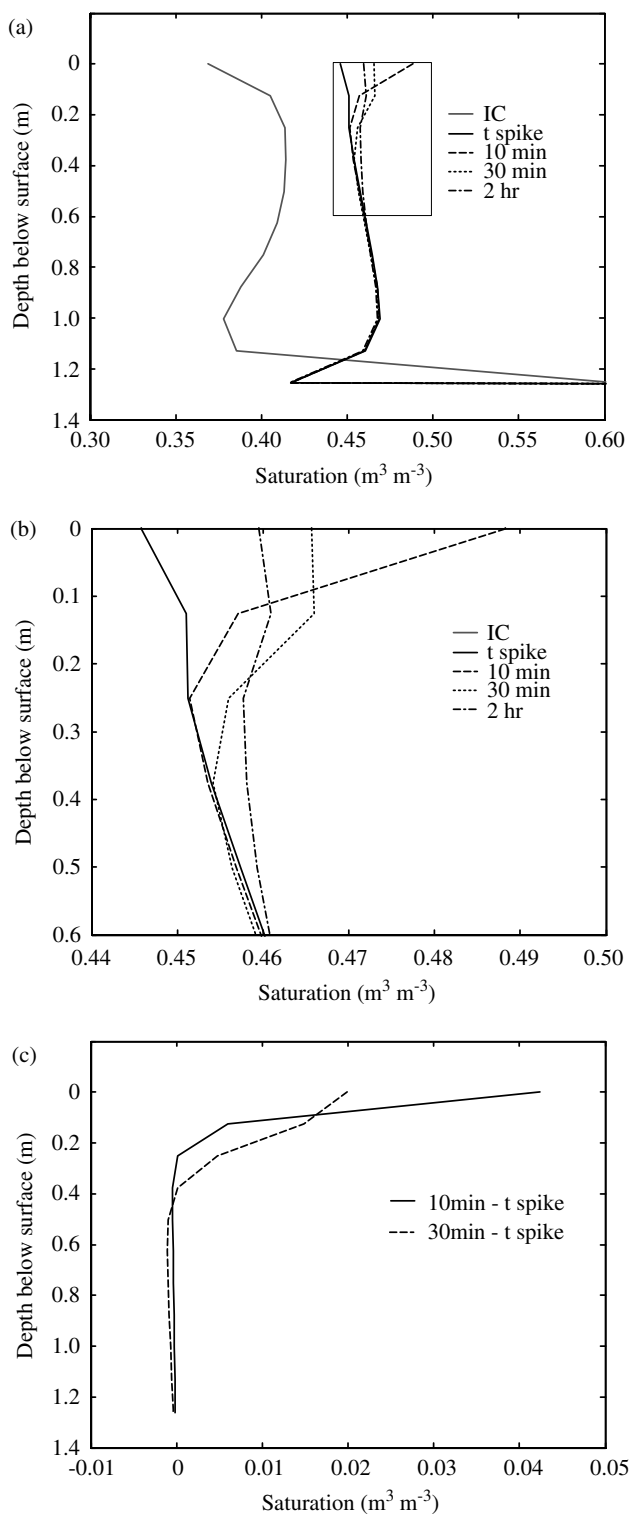


Figure 4. (a) Time snapshots of simulated saturation profiles with depth for the simulated monitoring points for the second CB1 sprinkling experiment initial conditions (IC), at the initiation of the natural rainfall rate spike, 10 min after the rainfall spike initiated (also the cessation of the rainfall spike), 30 min after the rainfall spike initiated, and 2 h after the rainfall spike initiated. (b) Subset of the profiles shown in (a); note that the box in (a) shows the depth range of the subset. (c) Depth profiles of the differences between the saturations at the simulated monitoring points at the rainfall spike initiation and the time snapshots from 10 and 30 min after the rainfall spike

investigations (e.g. Smith, 1983; Beven, 1989b; Torres *et al.*, 1998; Williams *et al.*, 2002; Renshaw *et al.*, 2003;

Meyles *et al.*, 2006); specifically, rainfall rate spikes, storage, and steep hydraulic conductivity functions each contribute to rapid hydrologic response in the variably saturated near surface. The simulation results reported herein provide a first cut illustration of the levels of spatial discretization and temporal resolution necessary for future measurement campaigns that purport to aid in the resolution of questions related to rapid hydrologic response within the near surface (e.g. testing whether Equation (3) is valid for CB1 type applications). If, as suggested by Torres (2002), models like InHM are incapable of simulating hydrologic response for certain situations where the Darcy–Buckingham continuum assumptions break down, it is clear, from the effort reported here, that much better temporal resolution is needed for discharge, pressure head, and soil water content observations for conclusive data-based assessments. The temporal scale for the type of response that potentially occurred at CB1 would be on the order of minutes to a precision of, for example, millimeters for pressure head. On the basis solely of the CB1 sprinkling experiments, it is our opinion that it is premature to even consider total abandonment of the distributed physics-based hydrologic-response simulation approach. The findings reported here echo the call from Kirchner *et al.* (2004) for better temporal resolution in hydrologic observations. If InHM can adequately simulate the rapid hydrologic response, then the simulations reported herein provide an upper bound for the temporal discretization necessary for capturing rapid hydrologic response.

Smith (1983) noted that the velocity limit of the wetting front is provided by:

$$v(\theta) = \frac{dK(\theta)}{d(\theta)} \quad (7)$$

where  $\theta$  is soil water content [ $L^3 L^{-3}$ ]. Equation (7) is an estimate of the maximum possible wetting front velocity. The situation where the wetting front velocity will be greatest is where  $K(\theta)$  has the largest slope and storage is minimal. This maximum velocity should occur on the *wet side* of the specific moisture capacity curve (i.e.  $C(\psi)$ ) peak, but before the air-entry pressure. Figures 5(a) and (b) show, respectively, the relatively steep, nonhysteretic soil water retention and hydraulic conductivity functions for a loamy sand. The characteristic curves in Figure 5(a) and (b) were generated with the van Genuchten (1980) approach, parameterized from the Carsel and Parrish (1988) database. Figure 5(c) shows the specific moisture capacity curve, derived from the soil water retention curve. In Figure 5, the maximum velocity should occur for pressure heads between  $-0.05$  and  $-0.02$  m. An experiment, well beyond the scope of this briefing, to examine the maximum rate of hydrologic response for the soil depicted in Figure 5 would need to be irrigated until past the  $C(\psi)$  peak, then the irrigation spike increased. The temporal and spatial discretization of measurements necessary to capture the response could be gleaned from numerical simulations such as the ones reported here

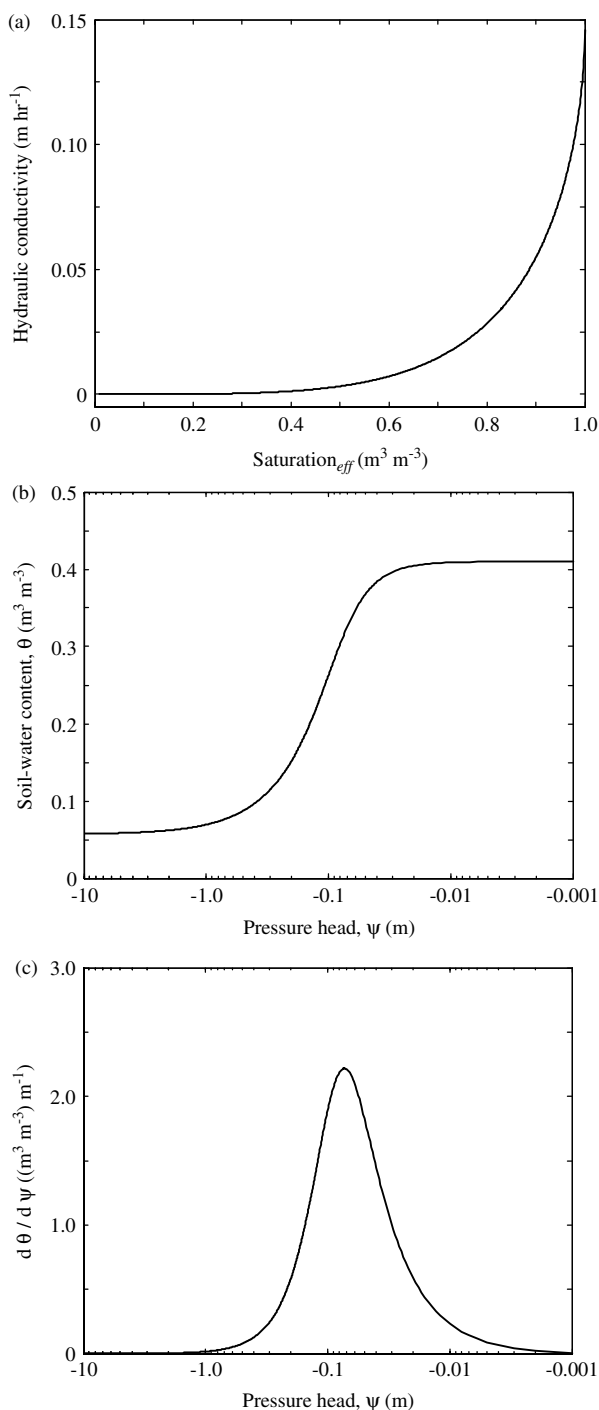


Figure 5. Characteristic curves for a loamy sand generated with the van Genuchten (1980) approach, parameterized from the Carsel and Parrish (1988) database. (a) Hydraulic conductivity function. (b) Nonhysteretic soil water retention curve. (c) Specific moisture capacity curve

or, for example, using kinematic wave approximations. It is important to note the paucity of high-quality soil water retention data at pressure heads  $< -0.1$  m. It is also possible that the van Genuchten (1980) relationships provide a less than perfect representation of soil water retention at pressure heads close to zero.

Finally, this short communication also illustrates the importance of nonlinear characteristic curves. Improvement in the representation of the characteristic curves

(see Held and Celia, 2001; Hassanizadeh *et al.*, 2002; Rasmussen, 2005) for applications of physics-based hydrologic-response models like InHM will further improve the simulation of rapid hydrologic response in the variably saturated near surface such as has been observed at CB1.

### Acknowledgements

The effort reported here was supported by National Science Foundation grant EAR-0409133. The developer of InHM is our long-time collaborator Joel VanderKwaak. The CB1 data was the result of heroic field efforts by Suzanne Anderson, Bill Dietrich, David Montgomery, and Ray Torres. The many discussions with Ben Mirus, Chris Heppner, and Steve Loheide, focused on rapid hydrologic response, are greatly appreciated. Finally, we are grateful to John Nimmo and an anonymous reviewer for their thoughtful comments on an earlier version of the manuscript.

### References

- Anderson SP, Dietrich WE. 2001. Chemical weathering and runoff chemistry in a steep headwater catchment. *Hydrological Processes* **15**: 1791–1815.
- Anderson SP, Dietrich WE, Brimhall GH. 2002. Weathering profiles, mass-balance analysis, and rates of solute loss: Linkages between weathering and erosion in a small, steep catchment. *Geological Society of America Bulletin* **114**: 1143–1158.
- Anderson SP, Dietrich WE, Torres R, Montgomery DR, Loague K. 1997a. Concentration discharge relationships in runoff from a steep, unchanneled catchment. *Water Resources Research* **33**: 211–225.
- Anderson SP, Dietrich WE, Montgomery DR, Torres R, Conrad ME, Loague K. 1997b. Subsurface flowpaths in a steep, unchanneled catchment. *Water Resources Research* **33**: 2637–2653.
- Beven K. 1981. Kinematic subsurface stormflow. *Water Resources Research* **17**: 1419–1424.
- Beven K. 1982. On subsurface stormflow: predictions with simple kinematic theory for saturated and unsaturated flows. *Water Resources Research* **18**: 1627–1633.
- Beven K. 1989a. Changing ideas in hydrology—the case of physically-based models. *Journal of Hydrology* **105**: 157–172.
- Beven K. 1989b. Interflow. In *Unsaturated Flow in Hydrologic Modeling: Theory and Practice*, Morel-Seytoux HJ (ed.). Kluwer Academic Publishers: Dordrecht.
- Beven K. 2004. Robert E. Horton's perceptual model of infiltration processes. *Hydrological Processes* **18**: 3447–3460.
- Beven K. 2006. A manifesto for the equifinality thesis. *Journal of Hydrology* **320**: 18–36.
- Beven KJ, Germann P. 1982. Macropores and water flow in soils. *Water Resources Research* **18**: 1311–1325.
- Carsel RF, Parrish RS. 1988. Developing joint probability distributions of soil water retention characteristics. *Water Resources Research* **24**: 755–769.
- Charbeneau RJ. 1984. Kinematic models for soil moisture and solute transport. *Water Resources Research* **20**: 699–706.
- Clothier BE. 2002. Rapid and far-reaching transport through structured soils. *Hydrological Processes* **16**: 1321–1323.
- Colbeck SC. 1972. A theory of water percolation in snow. *Journal of Glaciology* **11**: 369–385.
- Ebel BA, Loague K. 2006. Physics-based hydrologic response simulation: Seeing through the fog of equifinality. *Hydrological Processes* **20**: 2887–2900.

- Ebel BA, Loague K, Montgomery DR, Dietrich WE. 2007a. Physics-based continuous simulation of long-term near-surface hydrologic response for the Coos Bay experimental catchment. *Water Resources Research* (in press).
- Ebel BA, Loague K, Dietrich WE, Montgomery DR, Torres R, Anderson SP, Giambelluca TW. 2007b. Near-surface hydrologic response for a steep, unchanneled catchment near Coos Bay, Oregon: 1. Sprinkling experiments. *American Journal of Science* **307**: 678–708.
- Ebel BA, Loague K, VanderKwaak JE, Dietrich WE, Montgomery DR, Torres R, Anderson SP. 2007c. Near-surface hydrologic response for a steep, unchanneled catchment near Coos Bay, Oregon: 2. Comprehensive physics-based simulations. *American Journal of Science* **307**: 709–748.
- Hassanizadeh SM, Celia MA, Dahle HK. 2002. Dynamic effects in the capillary pressure—saturation relationship and their impacts on unsaturated flow. *Vadose Zone Hydrology* **1**: 38–57.
- Held RJ, Celia MA. 2001. Pore-scale modeling extension of constitutive relationships in the range of residual saturations. *Water Resources Research* **37**: 165–170.
- Heppner CS, Loague K, VanderKwaak JE. 2007. Long-term InHM simulations of hydrologic response and sediment transport for the R-5 catchment. *Earth Surface Processes and Landforms* **32**: 1273–1292. DOI: 10.1002/esp.1474.
- Heppner CS, Ran Q, VanderKwaak JE, Loague K. 2006. Adding sediment transport to the Integrated Hydrology Model (InHM): development and testing. *Advances in Water Resources* **9**: 930–943.
- Horton RE. 1940. An approach toward the physical interpretation of infiltration-capacity. *Soil Science Society of America Journal* **5**: 399–417.
- Jones JP, Sudicky EA, Brookfield AE, Park Y-J. 2006. An assessment of the tracer-based approach to quantifying groundwater contributions to streamflow. *Water Resources Research* **42**: W02407, DOI:10.1029/2005WR004130.
- Kirchner JW, Feng X, Neal C, Robson AJ. 2004. The fine structure of water-quality dynamics: the (high-frequency) wave of the future. *Hydrological Processes* **18**: 1353–1359.
- Loague K, VanderKwaak JE. 2004. Physics-based hydrologic response simulation: platinum bridge, 1958 Edsel, or useful tool. *Hydrological Processes* **18**: 2949–2956.
- Loague K, Heppner CS, Abrams RH, VanderKwaak JE, Carr AE, Ebel BA. 2005. Further testing of the Integrated Hydrology Model (InHM): Event-based simulations for a small rangeland catchment located near Chickasha, Oklahoma. *Hydrological Processes* **19**: 1373–1398.
- Loague K, Heppner CS, Mirus BB, Ebel BA, Ran Q, Carr AE, BeVilleville SH, VanderKwaak JE. 2006. Physics-based hydrologic-response simulation: foundation for hydroecology and hydrogeomorphology. *Hydrological Processes* **20**: 1231–1237.
- Meyles EW, Williams AG, Ternan JL, Anderson JM, Dowd JF. 2006. The influence of grazing on vegetation, soil properties and stream discharge in a small Dartmoor catchment, southwest England, UK. *Earth Surface Processes and Landforms* **31**: 622–631.
- Mirus BB, Ebel BA, Loague K, Wemple BC. 2007. Simulated effect of a forest road on near-surface hydrologic response: redux. *Earth Surface Processes and Landforms* **32**: 126–142.
- Montgomery DR, Dietrich WE. 2002. Runoff generation in a steep, soil-mantled landscape. *Water Resources Research* **38**: 1168, DOI:10.1029/2001WR000822.
- Montgomery DR, Dietrich WE, Heffner JT. 2002. Piezometric response in shallow bedrock at CB1: implication for runoff generation and landsliding. *Water Resources Research* **38**: 1274, DOI:10.1029/2002WR001429.
- Montgomery DR, Dietrich WE, Torres R, Anderson SP, Heffner JT, Loague K. 1997. Hydrologic response of a steep, unchanneled valley to natural and applied rainfall. *Water Resources Research* **33**: 91–109.
- Nimmo JR. 2007. Simple predictions of maximum transport rate in unsaturated soil and rock. *Water Resources Research* **43**: W05426, DOI:10.1029/2006WR005372.
- Ran Q, Heppner CH, VanderKwaak JE, Loague K. 2007. Further testing of the Integrated Hydrology Model (InHM): multiple-species sediment transport. *Hydrological Processes* **21**: 1522–1531.
- Rasmussen TC. 2005. Rapid hydrologic responses due to dynamic contact angles. *Eos Transactions-American Geophysical Union* **86**(52): Fall Meeting Supplement, Abstract H24A-02: F773.
- Rasmussen TC, Baldwin RH, Dowd JF, Williams AG. 2000. Tracer vs. pressure wave velocities through unsaturated saprolite. *Soil Science Society of America Journal* **64**: 75–85.
- Renshaw CE, Feng X, Sinclair KJ, Dums RH. 2003. The use of stream flow routing for direct channel precipitation with isotopically-based hydrograph separations: the role of new water in stormflow generation. *Journal of Hydrology* **273**: 205–216.
- Sieck LC, Burges SJ, Steiner M. 2007. Challenges in obtaining reliable measurements of point rainfall. *Water Resources Research* **43**: W01420, DOI:10.1029/2005WR004519.
- Smerdon BD, Medoza CA, Devito KJ. 2007. Simulations of fully coupled lake-groundwater exchange in a subhumid climate with an integrated hydrologic model. *Water Resources Research* **43**: W01416, DOI: 10.1029/2006WR005137.
- Smith RE. 1983. Approximate soil water movement by kinematic characteristics. *Soil Science Society of America Journal* **47**: 3–8.
- Smith RE, Smettem KRJ, Broadbridge P, Woolhiser DA. 2002. *Infiltration Theory for Hydrologic Applications*. American Geophysical Union: Washington, DC: 212.
- Torres R. 2002. A threshold condition for soil-water transport. *Hydrological Processes* **16**: 2703–2706.
- Torres R, Dietrich WE, Montgomery DR, Anderson SP, Loague K. 1998. Unsaturated zone processes and the hydrologic response of a steep, unchanneled catchment. *Water Resources Research* **34**: 1865–1879.
- VanderKwaak JE. 1999. Numerical simulation of flow and chemical transport in integrated surface-subsurface hydrologic systems, PhD dissertation, University of Waterloo, Waterloo.
- VanderKwaak JE, Loague K. 2001. Hydrologic-response simulations for the R-5 catchment with a comprehensive physics-based model. *Water Resources Research* **37**: 999–1013.
- van Genuchten MTh. 1980. A closed-form equation for predicting the hydraulic conductivity of unsaturated soils. *Soil Science Society of America Proceedings* **44**: 892–898.
- Warrick AW, Biggar JW, Nielsen DR. 1971. Simultaneous solute and water transfer for an unsaturated soil. *Water Resources Research* **7**: 1216–1225.
- Williams AG, Dowd JF, Meyles EW. 2002. A new interpretation of kinematic stormflow generation. *Hydrological Processes* **16**: 2791–2803.